

Characterizing asymmetric and bimodal long-term financial return distributions through quantum walks

Stijn De Backer^a, Luis E. C. Rocha^{a,b}, Jan Ryckebusch^a, Koen Schoors^b

^a*Department of Physics and Astronomy, Ghent University, Ghent, Belgium*

^b*Department of Economics, Ghent University, Ghent, Belgium*

Abstract

The analysis of logarithmic return distributions defined over large time scales is crucial for understanding the long-term dynamics of asset price movements. For large time scales of the order of two trading years, the anticipated Gaussian behavior of the returns often does not emerge, and their distributions often exhibit a high level of asymmetry and bimodality. These features are inadequately captured by the majority of classical models to address financial time series and return distributions. In the presented analysis, we use a model based on the discrete-time quantum walk to characterize the observed asymmetry and bimodality. The quantum walk distinguishes itself from a classical diffusion process by the occurrence of interference effects, which allows for the generation of bimodal and asymmetric probability distributions. By capturing the broader trends and patterns that emerge over extended periods, this analysis complements traditional short-term models and offers opportunities to more accurately describe the probabilistic structure underlying long-term financial decisions.

Keywords: financial return distributions, quantum walks, long-term asset price dynamics, financial algorithm design

PACS: 89.65.Gh

2020 MSC: 91B80

1. Introduction

The analysis of financial time series is fundamental to understanding market behavior, risk assessment, and economic trends, making it a key element of research in both finance and econophysics. The first model to describe the dynamics of financial time series was developed by Bachelier in 1900 [1], in which the movements of asset prices were governed by a classical random walk as underlying stochastic process. This model was unable to capture fat-tailed return distributions and the corresponding extreme price changes. Bachelier noted these extreme price fluctuations but categorized them as outliers that did not deserve further attention [2]. In 1963, Mandelbrot proposed Lévy stable distributions as a model for financial return distributions, which included the possibility to address fat tails [3]. Since then, a plethora of models for financial time series and return distributions has been proposed [4, 5, 6, 7, 8, 9, 10, 11, 12, 13, 14, 15, 16, 17, 18, 19, 20], each having their own capabilities, limitations, and complexity level.

Email address: `stijn.debacker@ugent.be` (Stijn De Backer)

Preprint submitted to Elsevier

May 29, 2025

The distributions of returns defined over time scales ranging from 15 seconds to a few days can often be adequately fitted with power laws [6, 7], reflecting their characteristic fat tails for these relatively short time scales. Alternative and more advanced models to fit these types of distributions include stretched exponentials and log-Weibull distributions [20]. Return distributions for small values of the time scale have been the subject of extensive data analysis efforts.

Return distributions defined over large time scales of the order of months and years are a rather underexplored topic in the literature [21]. It is commonly assumed that for increasing time scales, return distributions converge toward a Gaussian distribution [22, 23, 24, 25, 26]. In this paper, however, it is shown that for time scales approaching hundreds of trading days, the Gaussian behavior rarely emerges. Instead, one frequently observes non-Gaussian shapes, often exhibiting a high level of asymmetry and even bimodality. This behavior over larger time scales is not well captured by existing models.

Studying return distributions over large time scales provides insights into the long-term dynamics of asset price movements. Such an analysis is particularly relevant for applications like option pricing, where the long-term behavior of asset prices plays an important role in valuing derivatives. By identifying patterns in long-term return distributions, this study complements traditional short-term models for return distributions and can deepen our understanding of the probabilistic structure underlying long-term financial decisions.

In this paper, we apply a model for financial time series and return distributions based on the discrete-time quantum walk algorithm [27]. This model is used to characterize the observed asymmetry and bimodality in the return distributions of a variety of financial assets. In contrast to a classical random walk, the discrete-time quantum walk features interference effects in the diffusion process, which allows for the generation of bimodal and asymmetric probability distributions. We aim to model the asymmetry and bimodality in the financial return distributions by leveraging the interference effects inherent in the quantum walk algorithm. In this respect, it represents one of the simplest possible extensions of a classical diffusion process incorporating quantum interference effects. Introducing decoherence into the quantum walk causes it to collapse to a classical random walk [27, 28, 29, 30, 31, 32, 33, 34], thus the quantum walk model for financial time series can be regarded as an extension of a classical model based on geometric Brownian motion [4].

This paper applies the quantum walk model to financial assets with long-term return distributions that exhibit a clear level of asymmetry or bimodality. These features are poorly described by classical models. In this way, this work should be seen as a further data-driven motivation for the quantum walk based model for return distributions proposed in Ref. [27]. It is important to clarify that modeling asset price evolution using a quantum model does not imply that the dynamics of asset prices should be interpreted as a quantum process. Rather, the model serves as a versatile framework to capture non-Gaussian features of asset price dynamics. In this way, it adds to the diversity of existing methodologies and offers an alternative perspective on modeling financial time series and return distributions.

In the analysis presented here, we focus on the quantum walk algorithm without decoherence effects, as methodologies to introduce decoherence differ in the way the quantum walk distributions gradually evolve toward those of a classical random walk for increasing decoherence rates [28, 29, 30, 31, 32, 33, 34]. Even for relatively low decoherence rates, the resulting distributions resemble classical ones and the distinctive features of quantum walk distributions are lost. Additionally, quantum walks with decoherence involve stochasticity, thus their resulting probability distributions cannot be determined exactly. In contrast, unitary quantum walks yield fully deterministic probability distributions.

The structure of this paper is as follows. In Section 2, we briefly revise the quantum walk algorithm and the associated model for financial time series and the corresponding return distributions. In Section 3, an analysis of empirical time series of asset prices illustrates the emergence of asymmetry and bimodality in distributions of returns defined over large time scales. Section 4 discusses how the quantum walk model can account for those distinctive features. In Subsection 4.1, we outline the methodology to fit empirical return distributions with probability distributions resulting from quantum walks. In Subsection 4.2, we present and discuss the results of the fitting procedure. Section 5 summarizes our main conclusions.

2. Quantum walk model

2.1. Discrete-time quantum walk

Before turning to the quantum walk model for financial time series, we briefly revise the quantum walk algorithm [35, 36, 37], focusing on the parameters that specify its dynamics and its initial conditions.

The state of the quantum walk system lies in a Hilbert space $\mathcal{H} \equiv \mathcal{H}_C \otimes \mathcal{H}_P$, where the two-dimensional coin space \mathcal{H}_C is spanned by the two spin-1/2 states

$$|\uparrow\rangle = \begin{pmatrix} 1 \\ 0 \end{pmatrix}, \quad |\downarrow\rangle = \begin{pmatrix} 0 \\ 1 \end{pmatrix}, \quad (1)$$

and the position space \mathcal{H}_P is spanned by a discrete set of the position basis states $\{|j \in \mathbb{Z}\rangle\}$. A quantum walk of n discrete time steps corresponds to applying the operator \widehat{V}^n to a given initial state $|\psi(n=0)\rangle$. The unitary operator \widehat{V} is defined as

$$\widehat{V} = \widehat{T} \cdot (\widehat{C} \otimes \widehat{\mathbb{I}}_P), \quad (2)$$

where \widehat{C} is the quantum coin toss operator in coin space, $\widehat{\mathbb{I}}_P$ is the unity operator in position space, and \widehat{T} is the conditional translation operator. The most general quantum coin toss operator \widehat{C} for a quantum walk initialized at position $j = 0$ is represented by the 2×2 matrix [27]

$$U_{\eta,\theta} = \begin{pmatrix} e^{i\eta} \cos \theta & \sin \theta \\ \sin \theta & -e^{-i\eta} \cos \theta \end{pmatrix}, \quad (3)$$

where the angles $\eta \in [0, 2\pi[$ and $\theta \in [0, \pi/2]$ are referred to as the coin parameters. The conditional translation operator \widehat{T} is defined by

$$\widehat{T} = \left[|\uparrow\rangle\langle\uparrow| \otimes \left(\sum_{j \in \mathbb{Z}} |j+1\rangle\langle j| \right) \right] + \left[|\downarrow\rangle\langle\downarrow| \otimes \left(\sum_{j \in \mathbb{Z}} |j-1\rangle\langle j| \right) \right], \quad (4)$$

and imposes a move to the right (left) for the up (down) component in each time step.

After n time steps, the system's state can be written as

$$|\psi(n)\rangle = \widehat{V}^n |\psi(n=0)\rangle = \sum_{j=-n}^{+n} (a_j(n) |\uparrow\rangle + b_j(n) |\downarrow\rangle) \otimes |j\rangle, \quad (5)$$

where the amplitudes $a_j(n)$ and $b_j(n)$ capture the contribution of the up and down components at position j . The occupation probability of position j after n discrete time steps is

$$P_j(n) = |\langle j | \psi(n) \rangle|^2 = |a_j(n)|^2 + |b_j(n)|^2. \quad (6)$$

Without loss of generality, the Bloch sphere representation can be used for the initial state

$$|\psi(n=0)\rangle = [\cos(\omega/2)|\uparrow\rangle + \exp(i\phi)\sin(\omega/2)|\downarrow\rangle] \otimes |j=0\rangle, \quad (7)$$

where $\phi \in [0, 2\pi[$ and $\omega \in [-\pi, \pi]$ are the initial condition parameters. By selectively tuning the quantum coin parameters (η, θ) of Eq. (3) and the initial condition parameters (ϕ, ω) of Eq. (7), asymmetric and bimodal probability distributions can be generated [27, 38].

In a quantum walk, all possible paths in position space evolve simultaneously, with interference occurring between them. This differs from a classical random walk, where the direction of the next step is decided at each time step. The randomness in a quantum walk only arises upon measurement, while the computation of its probability distribution (Eq. (6)) is fully deterministic.

2.2. Quantum walk model for financial time series

In the quantum walk model for financial time series, the asset price increments $dS = S(t + dt) - S(t)$ in a time interval dt are given by [27]

$$dS = \mu S(t)dt + \sigma S(t)[f(t)dQ(t)], \quad (8)$$

where $S(t)$ is the asset price at time t , μ is the rate of a general drift, σ is a volatility parameter, $Q(t)$ represents a discrete-time quantum walk process, and $f(t)$ is a function that controls the long-term diffusion properties of the asset price evolution. For example, by setting $f(t) \propto t^{-1/2}$, one can account for the ballistic diffusion property of the quantum walk [27].

A primary goal of this paper is to use quantum walk probability distributions to model logarithmic return distributions $P_{\Delta t}(g)$ of financial assets. The logarithmic return g of an asset S is defined as the difference in logarithmic price over a duration Δt

$$g \equiv g(t; \Delta t, S) = \log_e S(t + \Delta t) - \log_e S(t). \quad (9)$$

In the quantum walk model of Eq. (8), the drift parameter μ determines the horizontal shape-preserving translation of the logarithmic return distribution $P_{\Delta t}(g)$. The choice $\mu = 0$ corresponds to an asset price evolution purely governed by the quantum walk process $Q(t)$. When fitting an empirical $P_{\Delta t}(g)$ with a quantum walk distribution, the value of the product $\sigma f(\Delta t)$ can be seen as a rescaling factor for the range over which g extends. Specifically, $\sigma f(\Delta t)$ is chosen to match the scale of the quantum walk fit to that of the empirical return distribution $P_{\Delta t}(g)$. The precise fitting procedure is outlined in Subsection 4.1.

3. Identifying asymmetry and bimodality in return distributions

In this section, we discuss the changes in the overall shape of return distributions $P_{\Delta t}(g)$ if one increases the time scale Δt . We analyzed the time series of the opening price of 31 financial assets, including stocks and funds. The data were retrieved from <https://finance.yahoo.com/> on October 14, 2024. The assets were analyzed over a period of 30 calendar years, or over shorter periods if the data covered less than 30 calendar years. Non-trading days, such as weekend days and public holidays, are excluded from the analysis. Consecutive trading days (for example, a Friday followed by the next Monday) are treated as successive time points in the time series when computing the return distributions. Table A.2 in the appendix provides an overview of all analyzed assets, presenting their ticker, full name, sector, industry, and the end and start date of the time series.

The assets were selected based on the criterion that they exhibit pronounced asymmetry or bimodality in their return distribution at large Δt . We refer to time scales Δt as “large” from 100 trading days onwards. To investigate return distributions with $\Delta t \gtrsim 100$ trading days, assets with long-term data availability are required, thereby excluding assets that have only been on the market for a limited time. Additionally, we focus on assets that exhibit a pronounced level of bimodality or asymmetry in their return distributions at large time scales Δt . These selection criteria narrow the set of assets included in the analysis.

Fig. 1 displays waterfall plots of the $P_{\Delta t}(g)$ of six assets for increasing values of the time scale Δt . We restrict ourselves to $\Delta t \leq 504$ trading days as this corresponds to two trading years (one trading year equals 252 trading days). For $\Delta t = 1$ trading day, the distributions are sharply peaked and leptokurtic, which is a well-documented finding in the literature [12, 14, 15, 39, 40, 41, 42, 43]. For $\Delta t = 50$ trading days, the distributions transition toward a Gaussian-like shape. For $\Delta t > 50$ trading days, the $P_{\Delta t}(g)$ in Fig. 1 display clear bimodality, in particular for $\Delta t = 504$ trading days.

Several statistical tests have been proposed to discriminate between a unimodal and multimodal distribution [44, 45, 46, 47, 48]. Rather than merely determining whether a distribution $P(x)$ is bimodal or not, we wish to quantify the degree of bimodality of $P(x)$. Therefore, we introduce a bimodality measure $0 \leq \text{BM} \leq 1$ that satisfies the following two criteria. Firstly, it should adopt a large value if the two peaks are equally high, and if the probability distribution substantially drops between them. Secondly, BM should increase for larger separations between the two peaks. A definition that satisfies these criteria is (see Fig. 2 for an illustration of the notation conventions)

$$\text{BM} \equiv \left(\frac{P_{\max,2} - P_{\min}}{P_{\max,1}} \right) \times \left(\frac{\Delta x}{L_{\text{eff}}} \right), \quad (10)$$

where $P_{\max,1}$ and $P_{\max,2}$ are the probabilities at the modes (with $P_{\max,1} \geq P_{\max,2}$), P_{\min} is the minimal value of $P(x)$ between these two modes, Δx is the distance between the two modes, and the effective range L_{eff} is defined as the range that contains the central 95% of the probability, excluding the outermost 2.5% on each side of the distribution. The introduction of L_{eff} in Eq. (10) guarantees that the value of BM is not heavily impacted by the extreme events on either side of the distribution. As required, the first factor in Eq. (10) favors an equal height of the two peaks and a substantial drop in probability between them. The second factor favors a larger separation of the two peaks, corresponding to a larger contrast between the events associated with the two modes (two well-separated classes of events). Note that the measure satisfies $0 \leq \text{BM} \leq 1$, except in some pathological distributions where $\Delta x > L_{\text{eff}}$.

Fig. 3 displays the bimodality measure BM of Eq. (10) as a function of the time scale Δt of the return distributions for the six assets in Fig. 1. Upon determining the bimodality measure, we ensure that the global structure of the distribution is captured by binning $P_{\Delta t}(g)$ into about 20 bins to cover the full range of the returns, thereby maintaining a low resolution that prevents small local peaks from emerging. For distributions with only one local maximum, the bimodality is set to zero. For $\Delta t = 2$ trading years, the distributions tend to have a high value of the bimodality measure defined in Eq. (10). For example, the $P_{\Delta t=504}(g)$ of TEAM (Fig. 1(f)) has two classes in its long-term returns. Indeed, the bump at $g \approx 1$ corresponds with a substantial gain over two trading years, whereas the bump at $g \approx -0.5$ can be associated with a substantial loss.

In Fig. 4, we present a similar waterfall plot as in Fig. 1 for a different set of six selected assets. The return distributions with $\Delta t = 504$ trading days are non-Gaussian and have a pronounced level of asymmetry, albeit without being bimodal. For $\Delta t \leq 50$ trading days, the trends

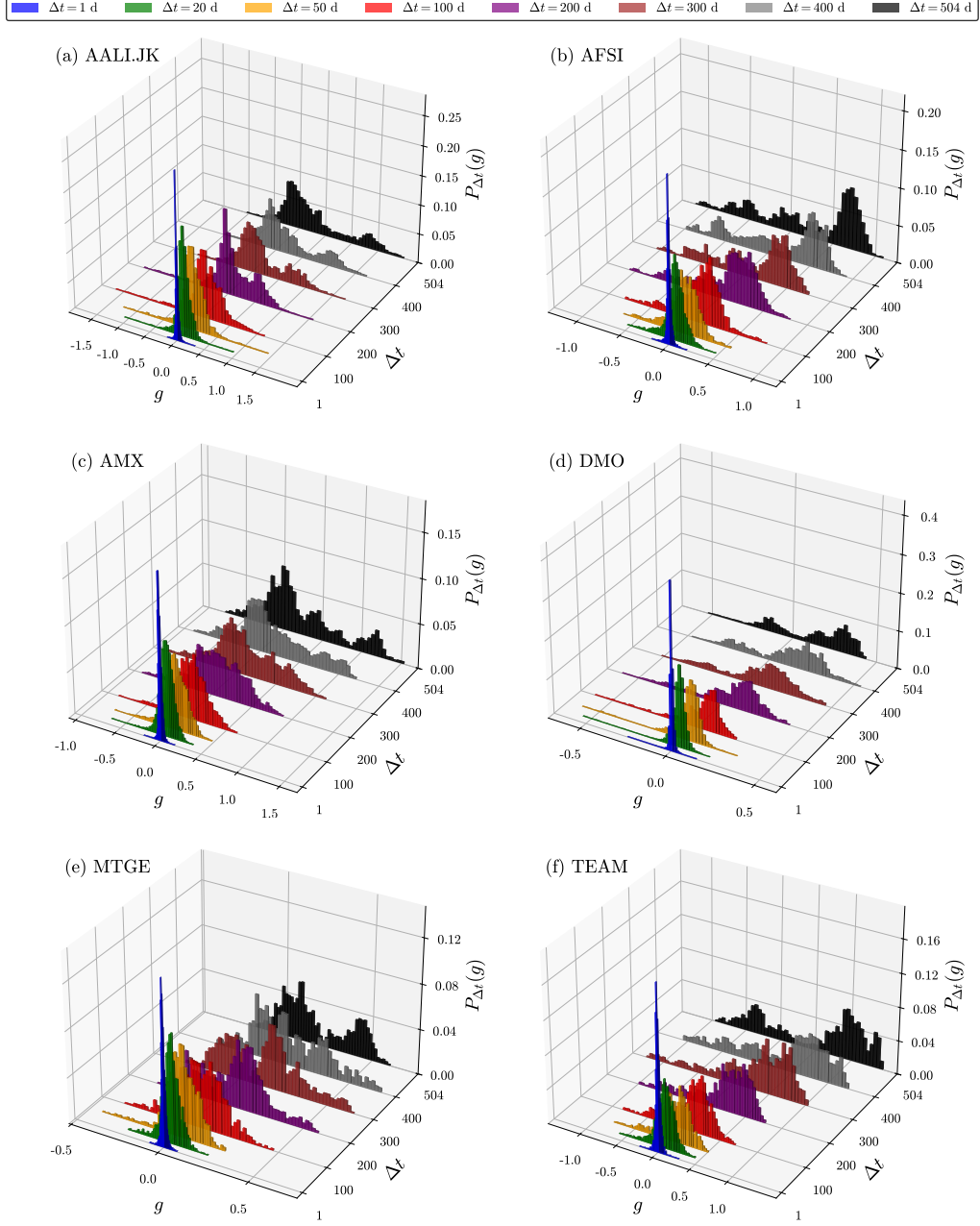


Figure 1: Waterfall plots of the return distribution $P_{\Delta t}(g)$ of six selected assets for increasing values of the time scale Δt (in trading days). The selection of the assets shown here (details in Table A.2) is based on $P_{\Delta t=504}(g)$ exhibiting a significant degree of bimodality.

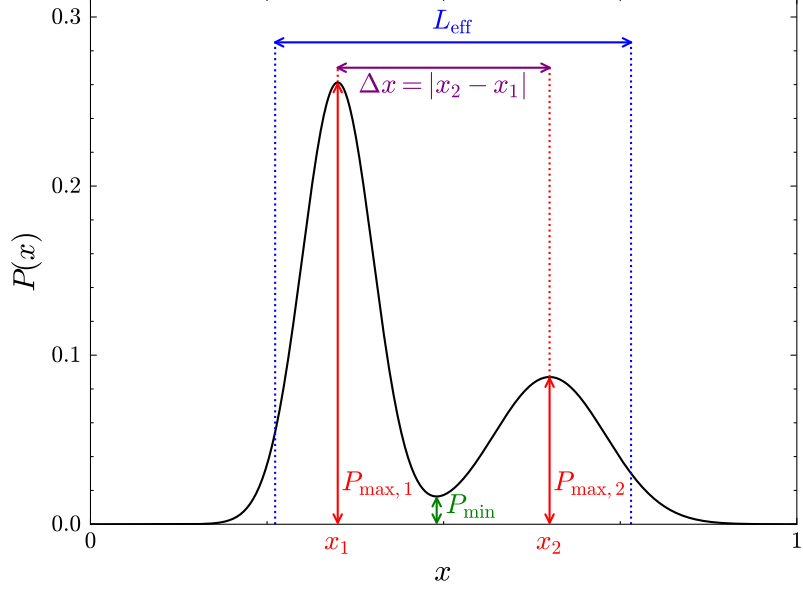


Figure 2: Illustration of the variables $P_{\max,1}$, $P_{\max,2}$, P_{\min} , Δx , and L_{eff} contained in the definition of the bimodality measure BM in Eq. (10).

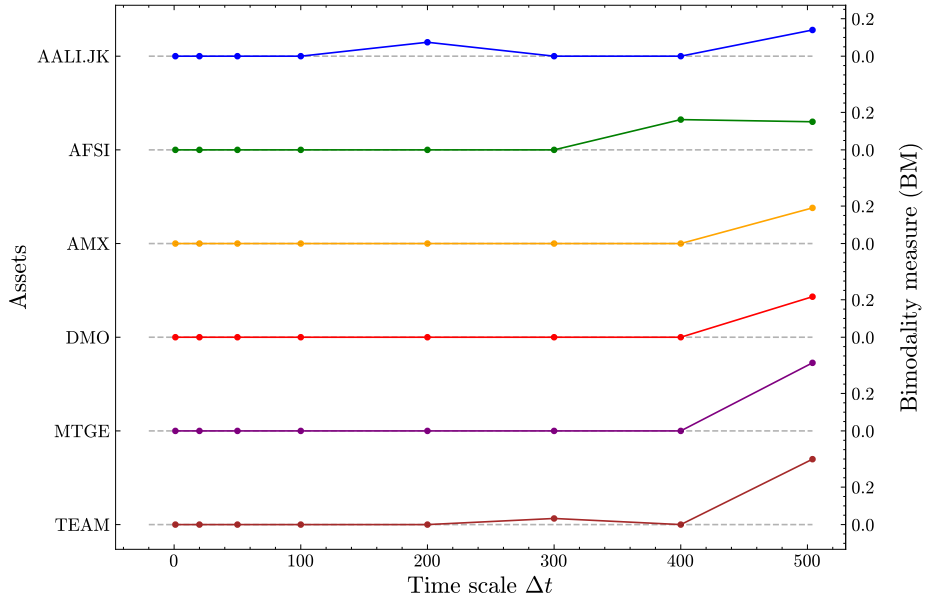


Figure 3: The Δt -dependence of the bimodality measure BM (Eq. (10)) of the return distributions $P_{\Delta t}(g)$ of Fig. 1.

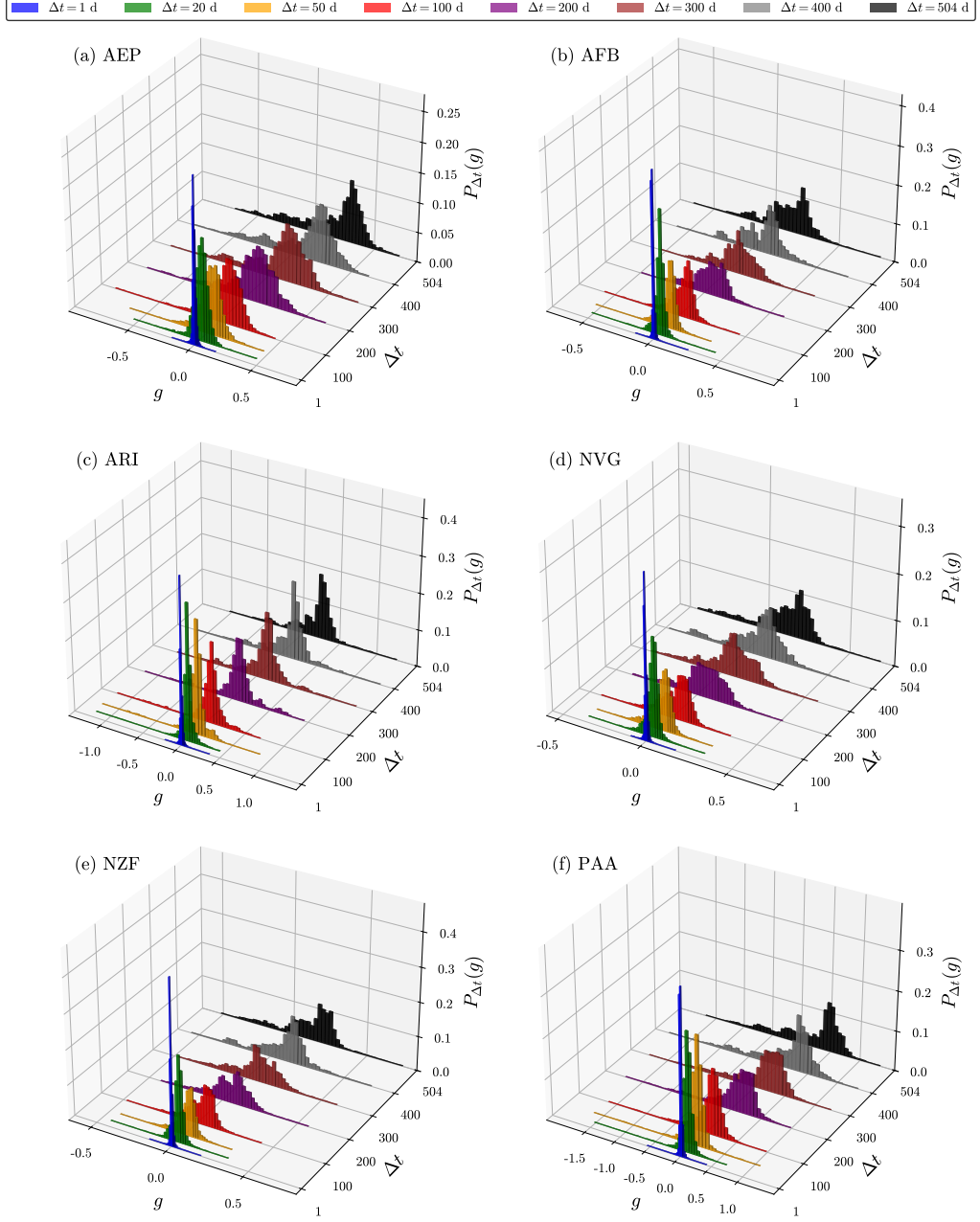


Figure 4: Waterfall plots of the return distribution $P_{\Delta t}(g)$ of six selected assets for increasing values of the time scale Δt (in trading days). The selection of the assets shown here (details in Table A.2) is based on $P_{\Delta t=504}(g)$ exhibiting a significant degree of asymmetry.

are similar to those observed in Fig. 1.

The level of asymmetry in a probability distribution can be quantified by the skewness

$$\gamma_1 = \frac{\kappa_3}{\kappa_2^{3/2}}, \quad (11)$$

where κ_i is the i th cumulant. In Fig. 5, the $|\gamma_1|$ of the return distributions in Fig. 4 is plotted as a function of the time scale Δt . We find that the distributions have a persistent level of asymmetry $|\gamma_1| \gtrsim 0.5$ across different time scales Δt .

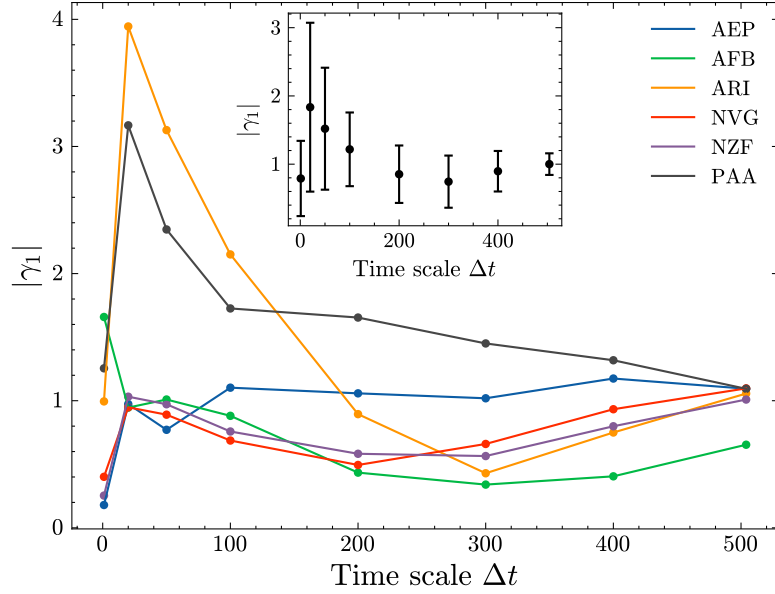


Figure 5: The Δt -dependence of the absolute value of the skewness of the return distributions $P_{\Delta t}(g)$ of Fig. 4. The inset figure shows the mean and standard deviation of $|\gamma_1|$ across the six assets.

Figs. 1, 3, 4 and 5 show that return distributions for $\Delta t \gtrsim 100$ trading days can deviate significantly from a Gaussian profile. Nevertheless, many models relying on long-term predictions of asset prices use a Wiener process or classical random walk as the underlying stochastic mechanism, inherently assuming Gaussian-distributed returns [4]. This assumption is exemplified in the Black-Scholes model for financial option pricing [5]. These models fail to adequately capture pronounced asymmetry and bimodality in long-term return distributions.

4. Quantum walk fits of long-term return distributions

In Subsection 4.2, the return distributions with $\Delta t = 2$ trading years of all 31 assets in the data set analyzed here will be fitted using probability distributions resulting from discrete-time quantum walks. The methodology for this is detailed in the forthcoming subsection.

4.1. Methodology

For each asset, we first computed the $P_{\Delta}(g)$ histogram with a small number of bins in order to capture the global structure of the distribution by suppressing the emergence of local spikes. The distributions are classified as unimodal or bimodal based on whether one or two local maxima are detected, adopting the methodology outlined in Section 3.

A key objective of our analysis is to determine the value of the quantum walk parameters ($\eta, \theta, \phi, \omega$) that yield the best fit to the empirical return distributions. Since the overall shape of a quantum walk probability distribution is not significantly impacted by varying the number of time steps n , n is set to 100. Only the width of the $P_j(n)$ of Eq. (6) is effectively affected by altering n , and this can be adjusted for by rescaling the position coordinates. A methodology based on a representative number of time steps n can capture the relevant features of the corresponding quantum walk probability distribution [27]. Moreover, fixing n reduces the number of fitting parameters, which is beneficial for the computational cost of the optimization process. The choice $n = 100$ strikes a balance between accuracy and computational cost. Indeed, if n were chosen too small, essential features of the quantum walk distribution could be lost, while a larger n would increase the computational cost of computing the quantum walk (which scales as $O(n^2)$) without introducing additional relevant features. In Subsection 4.2, we discuss how combining probability distributions from normally distributed values of n can further enhance the quantum walk model's performance in fitting return distributions. The robustness of our methodology with respect to the choices made for n will also be discussed in Subsection 4.2. Furthermore, quantum walk probability distributions exhibit spiky behavior due to local interference effects, which differs from what is typically observed in empirical data. To smooth the distinctive peaks, we aggregate each three consecutive positions j with non-zero probability in the quantum walk distribution into one single point, yielding a smoother probability distribution that can be used to fit empirical return distributions.

To determine the appropriate number of bins N_{bins} for the empirical return distribution used in the quantum walk fit, we first select a value such that, for a bimodal distribution, the two modes of the quantum walk fit align with the modes of the empirical distribution. For a unimodal asymmetric distribution, the mode and the long tail of the quantum walk fit are made to align smoothly with those of the empirical distribution. After selecting N_{bins} , we introduce two hyperparameters to further optimize the fit. The first hyperparameter adjusts the relative shift between the empirical and quantum walk distributions to assess whether this improves the quality of the fit. The second hyperparameter slightly varies the number of bins in the empirical histogram by a few (up to 4 bins) to investigate whether this adjustment enhances the fit performance. Finally, we impose that both the empirical distribution and the quantum walk fit use the same number of bins, for example by applying zero padding if necessary.

The goodness of fit is quantified by the mean absolute error (MAE)

$$\text{MAE} = \frac{1}{N_{\text{bins}}} \sum_{i=1}^{N_{\text{bins}}} |P_e(i) - P_{\text{QW}}(i)|, \quad (12)$$

where $P_e(i)$ and $P_{\text{QW}}(i)$ are the probabilities of the empirical return distribution and the quantum walk fit at bin i , respectively. Minimizing the MAE amounts to minimizing the surface between the empirical return distribution and the quantum walk fit. The search for the parameters ($\eta, \theta, \phi, \omega$) that minimize the MAE is performed using steepest-ascent hill climbing, which is a local search optimization algorithm [49]. The process begins with a large set of initial parameter guesses that cover the parameter space with low resolution. The parameter set yielding the lowest

MAE becomes the current estimate. In each iteration, the algorithm examines parameter values near the current estimate, progressively narrowing the search space for the optimal parameter values. The current estimate is updated at each iteration to reflect the best-performing parameter set. After a sufficient number of iterations, the optimal values of $(\eta, \theta, \phi, \omega)$ are identified to a precision of 0.0001 radians.

In the current analysis, we exclude decoherence effects from our quantum walk model. Our main motivation is that there is no unique way of introducing decoherence effects into the quantum walk algorithm [28, 29, 30, 31, 32, 33, 34]. Examples of methodologies to introduce decoherence are the stochastic disruption of links in the one-dimensional grid and the introduction of a random phase in the quantum coin [27]. The different approaches vary in how they cause the quantum walk distributions to gradually resemble those of a classical random walk as decoherence increases. Moreover, even at low levels of decoherence, the distributions already resemble classical ones, leading to the loss of the characteristic quantum walk features. Finally, due to the stochasticity introduced by decoherence, the resulting probability distributions cannot be determined exactly.

4.2. Results

In this subsection, we present the quantum walk fits for a broad selection of long-term empirical return distributions $P_{\Delta t}(g)$. In Fig. 6, the bimodal return distributions of Fig. 1 with $\Delta t = 2$ trading years are fitted using the methodology outlined in Subsection 4.1. In Fig. 7, the quantum walk fits of the asymmetric return distributions of Fig. 4 with $\Delta t = 2$ trading years are displayed. To keep the discussion concise, we highlight these 12 assets, while all remaining ones are succinctly discussed further below.

Although the fits show limitations, they capture the overall behavior of the distributions noticeably better than a Gaussian distribution. For Δt of the order of trading years, highly accurate fits are neither a realistic expectation nor the primary goal. Instead, the focus is on systematically capturing the key features of the distributions. The quantum walk fits tend to overestimate the height of the peaks, and sharply fall to nearly zero beyond them. As will be explained below, these issues can be addressed by a further adjustment in the handling of the number of time steps n in the fitting procedure.

The location of the initial position $|j = 0\rangle$ of the quantum walk (Eq. (7)) in Figs. 6 and 7 can be associated with the general drift term in the quantum walk model for financial time series (Eq. (8)). If the initial position is situated at $g \approx 0$, the drift term can be neglected ($\mu \approx 0$) and the quantum walk can describe the entire diffusion process of the asset price. This is a common feature of the asymmetric distributions in Fig. 7. However, this conclusion cannot be generalized to the bimodal distributions presented in Fig. 6.

The quantum walk model for return distributions distinguishes itself from other models by providing underlying dynamics for asset price evolution. Specifically, the parameters $(\eta, \theta, \phi, \omega)$ fix the dynamics and the initial condition of the quantum walk, rather than serving merely as morphological fit parameters of the $P_j(n = 100)$ of Eq. (6). The quantum walk model is suited for modeling bimodal return distributions, as the algorithm can accommodate the dynamics of two competing driving forces modeled by the quantum coin of Eq. (3) and the conditional translation operator of Eq. (4). A similar process can be observed in the asset price evolution in Fig. 1, where the price typically either rises or falls significantly over a large time interval Δt . These opposing tendencies contribute to the observed bimodality, making the quantum walk a compelling framework for describing this type of asset price behavior.

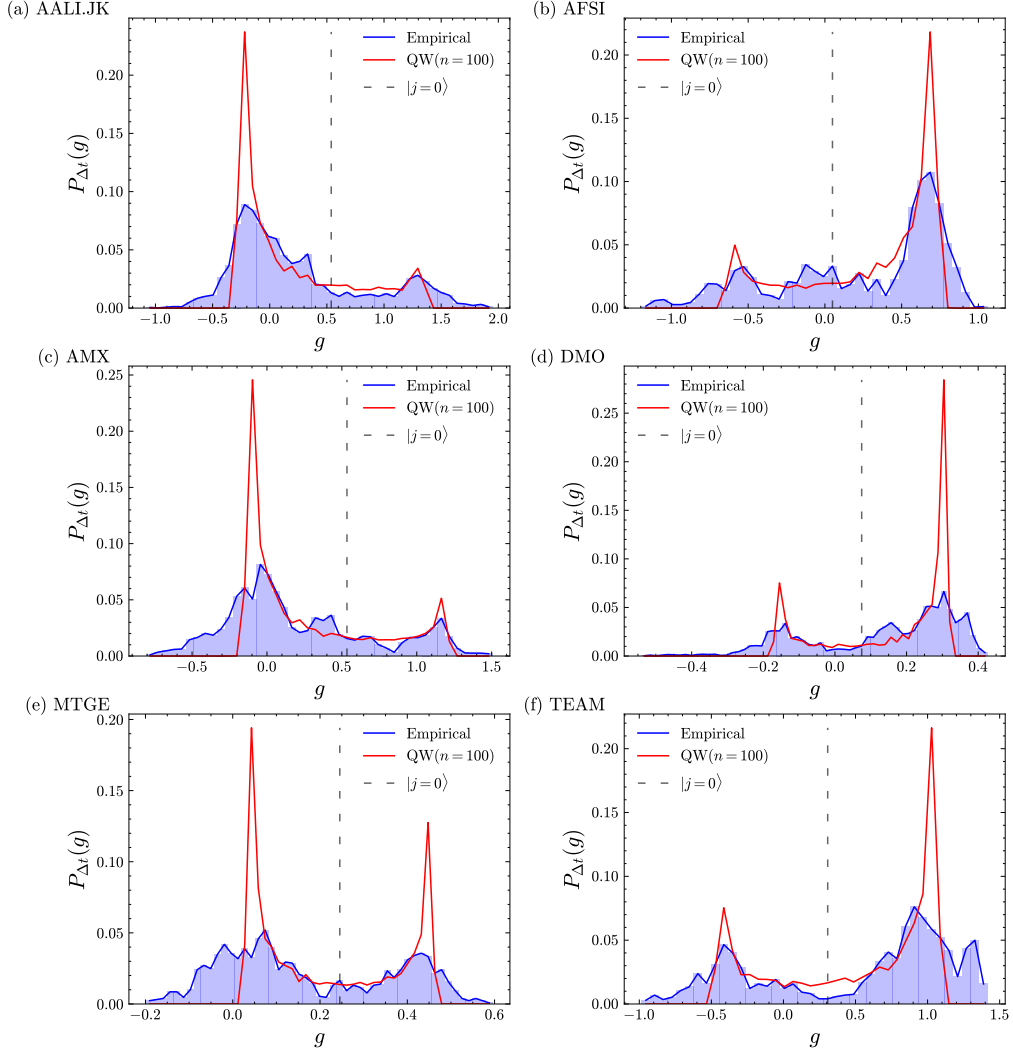


Figure 6: Quantum walk fit of the bimodal logarithmic return distribution $P_{\Delta t}(g)$ (with $\Delta t = 2$ trading years) for the six selected assets of Fig. 1. The number of time steps is set to $n = 100$. The vertical dashed line corresponds to the initial position $|j = 0\rangle$ of the quantum walk.

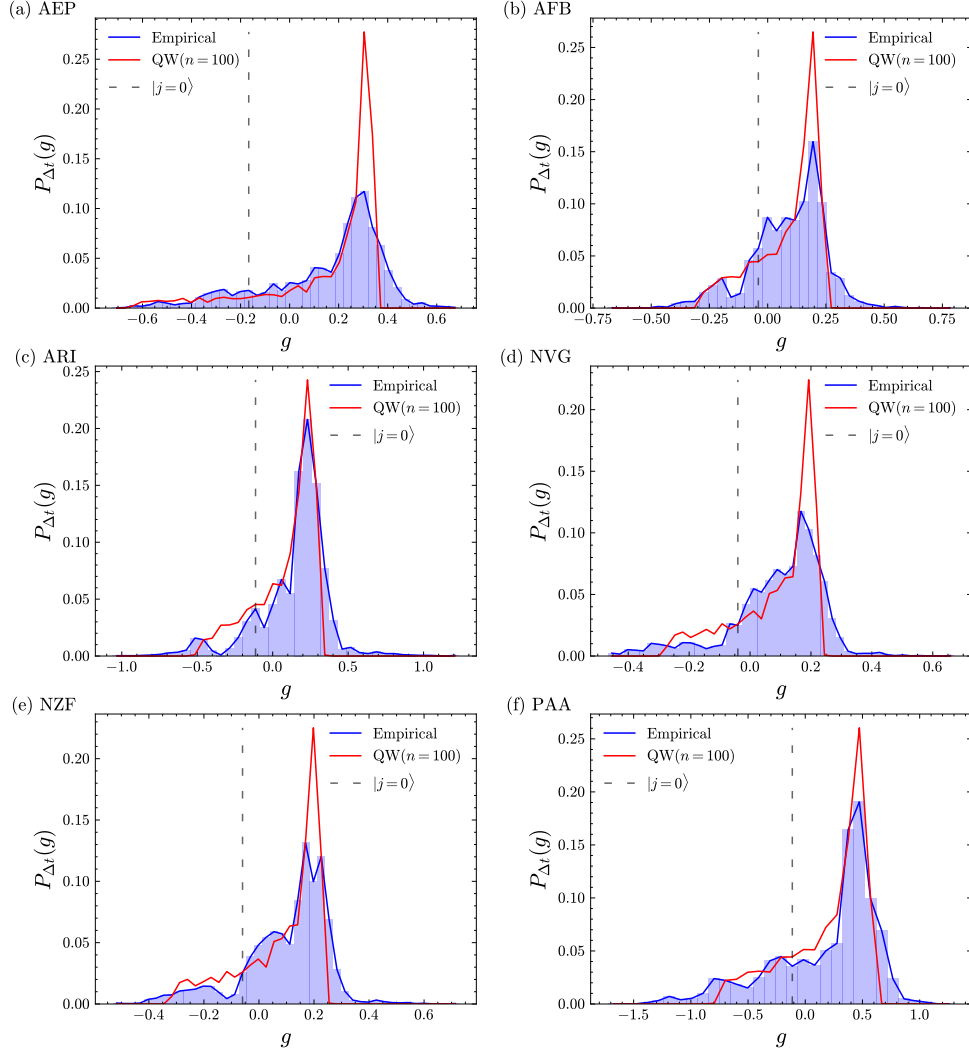


Figure 7: Quantum walk fit of the logarithmic return distribution $P_{\Delta t}(g)$ exhibiting considerable asymmetry (with $\Delta t = 2$ trading years) for the six selected assets of Fig. 4. The number of time steps is set to $n = 100$. The vertical dashed line corresponds to the initial position $|j = 0\rangle$ of the quantum walk.

Studying long-term return distributions is highly relevant for risk analysis, as it captures non-trivial characteristics that arise over extended time horizons. In particular, providing a good quantitative estimate of the pronounced negative tails of the empirical distributions in Fig. 7 and the negative bumps of the distributions in Fig. 6 is essential, as these relate to projected substantial losses.

The scatter plots in Fig. 8 display the fitted quantum coin parameters (η, θ) and initial condition parameters (ϕ, ω) for all 31 investigated assets (see Table A.2 for details), enabling the identification of regions of interest within the parameter space. For reference, limiting situations of the coin operator of Eq. (3) include the Hadamard coin with $(\eta = 0, \theta = \pi/4)$, the σ_z Pauli matrix with $(\eta = 0, \theta = 0)$, and the σ_x Pauli matrix with $(\eta = 0, \theta = \pi/2)$. Upon adopting the σ_z and σ_x as coin operator, the quantum walk model does not provide realistic return distributions, as reflected by the absence of points near these parameter values in the scatter plot. The coin parameter η consistently takes non-zero values, leading to complex numbers in the coin operator. There is a higher level of clustering in the coin parameter space (Fig. 8(a)) than in the initial condition parameter space (Fig. 8(b)). Since the coin parameters directly influence the dynamics of the quantum walk at each time step, their clustering suggests uniform dynamical properties across the investigated assets. Note that the initial condition parameters do not directly influence the dynamics after the start of the quantum walk. Moreover, the bimodal and asymmetric return distributions occupy different regions in the coin parameter space, linking these regions to specific asset price dynamics and distinct types of return distributions. A detailed investigation of the distribution and clustering of the fitted quantum walk parameters in parameter space (e.g., using principal component analysis or clustering algorithms) is a promising direction for future research, but falls outside the scope of the current analysis.

As noted earlier, the quantum walk fits in Figs. 6 and 7 overestimate the height of the peaks of the $P_{\Delta t}(g)$. Additionally, they abruptly drop to nearly zero beyond the peaks, unlike the empirical data. We explore the effect of smoothing the parameter n to resolve these discrepancies and substantially improve the quality of the quantum walk fits. Instead of taking a fixed number of time steps ($n = 100$), which corresponds to a delta distribution $\delta(n = 100)$, we average over 1000 quantum walk probability distributions where n is sampled from a normal distribution $\mathcal{N}(\mu = 100, \sigma^2 = 15^2)$. In this process, the sampled values of n are rounded to the nearest even integer. All other quantum walk parameters keep their values determined during the fit with $n = 100$.

The results of this adapted fitting methodology are displayed in Figs. 9 and 10 for the assets from Figs. 6 and 7, respectively. This modification effectively addresses the two issues previously noted. Indeed, the overestimation of peak heights is reduced, and the fitted distributions no longer abruptly drop to zero beyond their peaks, aligning more closely with the behavior of empirical data. Fig. 11 illustrates the effect of varying the mean and standard deviation of the normal distribution used to sample the number of time steps n . As a representative case, we consider the asset DMO, which has a bimodal return distribution (panel (d) in Fig. 9). Consistent with earlier discussions, these variations have limited impact on the results of the fitting procedure. As the essential features of the quantum walk fit remain unaffected, this observation supports the use of a fixed distribution $\mathcal{N}(\mu = 100, \sigma^2 = 15^2)$ in the main analysis.

In Fig. 10, we also present a Gaussian fit of the return distributions $P_{\Delta t}(g)$. Note that the quantum walk model more effectively captures the general shape of the return distributions compared to the Gaussian distribution. Attempts to fit the bimodal return distributions in Fig. 9 with a Gaussian distribution did not yield meaningful results. In Table 1, we list the MAE and the Kolmogorov–Smirnov (KS) statistic of the quantum walk fits (with $n \sim \mathcal{N}(\mu = 100, \sigma^2 = 15^2)$)

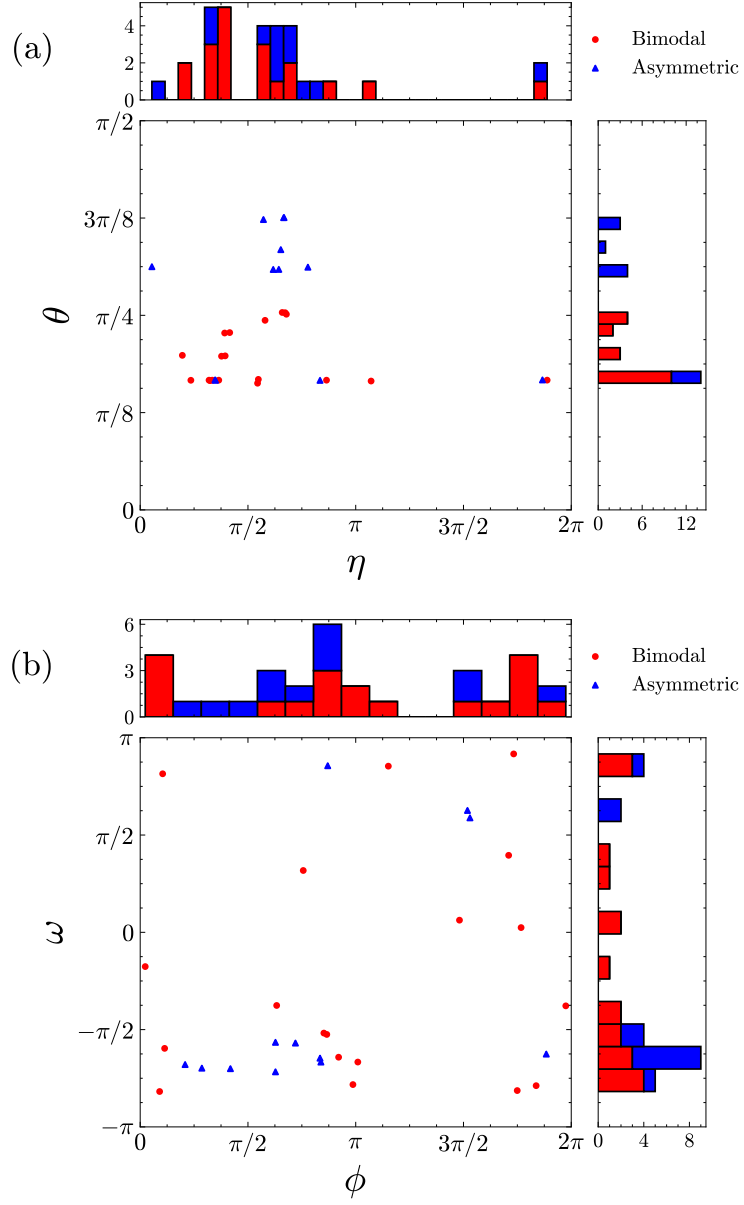


Figure 8: Scatter plots with marginal histograms of the fitted (a) quantum coin parameters (η, θ) and (b) initial condition parameters (ϕ, ω) for all 31 analyzed assets ($\Delta t = 2$ trading years). Bimodal and asymmetric return distributions are distinguished using different marker styles.

and the Gaussian fits for the distributions shown in Figs. 9 and 10. Except for the cases of ARI and NVG, the MAE of the quantum walk fit is lower than for the Gaussian fit, indicating a better characterization of the return distribution. Moreover, across all bimodal distributions, the KS statistic is consistently lower for the quantum walk fit compared to the Gaussian fit. These results underscore the shortcomings of the classical model and the superior overall performance of the quantum walk model in characterizing asymmetric and bimodal return distributions.

Asset	MAE (10^{-2})		KS (10^{-1})	
	QW ($n \sim \mathcal{N}$)	Gaussian	QW ($n \sim \mathcal{N}$)	Gaussian
AALIJK	0.640	-	0.661	-
AEP	0.524	0.964	0.456	2.953
AFB	0.813	0.899	0.908	1.191
AFSI	0.881	-	0.835	-
AMX	0.844	-	1.241	-
ARI	1.170	0.818	2.089	2.368
DMO	0.729	-	0.997	-
MTGE	0.906	-	1.999	-
NVG	0.757	0.745	0.777	1.380
NZF	0.774	0.918	1.172	1.775
PAA	1.209	1.452	1.309	3.414
TEAM	0.965	-	1.062	-

Table 1: MAE and KS statistic of the quantum walk fit (with $n \sim \mathcal{N}(\mu = 100, \sigma^2 = 15^2)$) and the Gaussian fit of the return distributions presented in Figs. 9 and 10. The lack of an appropriate Gaussian fit for the bimodal distributions is reflected by a hyphen for the MAE and KS statistic.

The results in Figs. 9 and 10 demonstrate the potential of the quantum walk model to capture key characteristics of long-term return distributions and the diffusion process of asset prices. Discrete-time quantum walks have been proposed earlier in a model for financial option pricing [50, 51, 52]. In this option pricing model, the probability distributions resulting from a quantum walk with the Hadamard coin and the symmetric initial state $|\psi(n=0)\rangle = 1/\sqrt{2}(|\uparrow\rangle + i|\downarrow\rangle) \otimes |j=0\rangle$ were used to represent economic agents' projections on the future value of the underlying asset. Our data analysis reinforces the assumptions of this model, as the occasional bimodal characteristics in long-term return distributions are incorporated into the option pricing model. Moreover, the results above illustrate that our quantum walk model offers an adequate characterization of bimodal return distributions, further corroborating the viability of the quantum walk-based option pricing model.

5. Conclusions

We analyzed asset price variations over extended periods using a model based on the discrete-time quantum walk, demonstrating its ability to capture specific empirical characteristics more effectively than a Gaussian model. We provided evidence for the emergence of bimodality and asymmetry in return distributions defined over time scales exceeding several months. The latter remain a relatively underexplored topic in econophysics and econometrics, despite their importance for models involving long-term predictions of asset prices and long-term risk assessment.

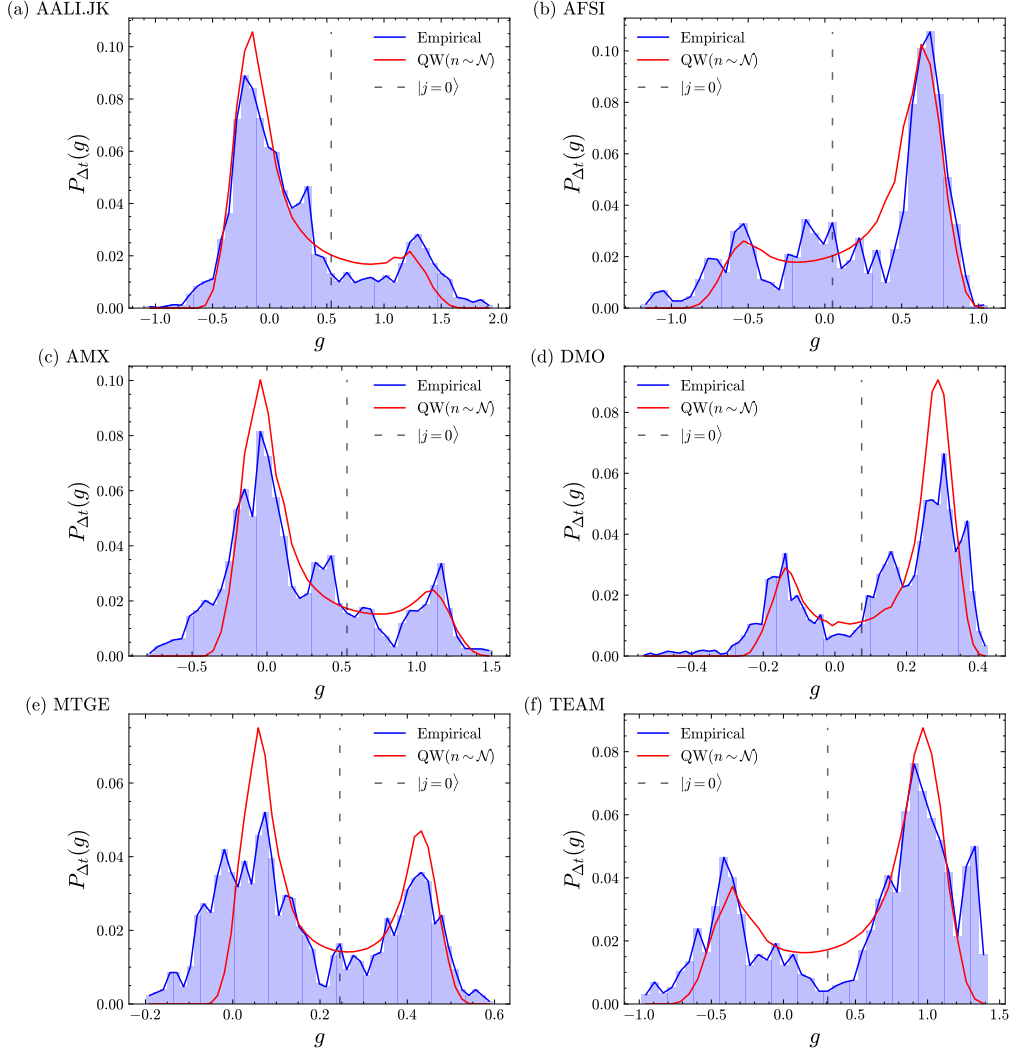


Figure 9: Quantum walk fit of the bimodal logarithmic return distribution $P_{\Delta t}(g)$ (with $\Delta t = 2$ trading years) for the six selected assets of Fig. 1. The number of time steps n is distributed according to a normal distribution $\mathcal{N}(\mu = 100, \sigma^2 = 15^2)$. The vertical dashed line corresponds to the initial position $|j = 0\rangle$ of the quantum walk.

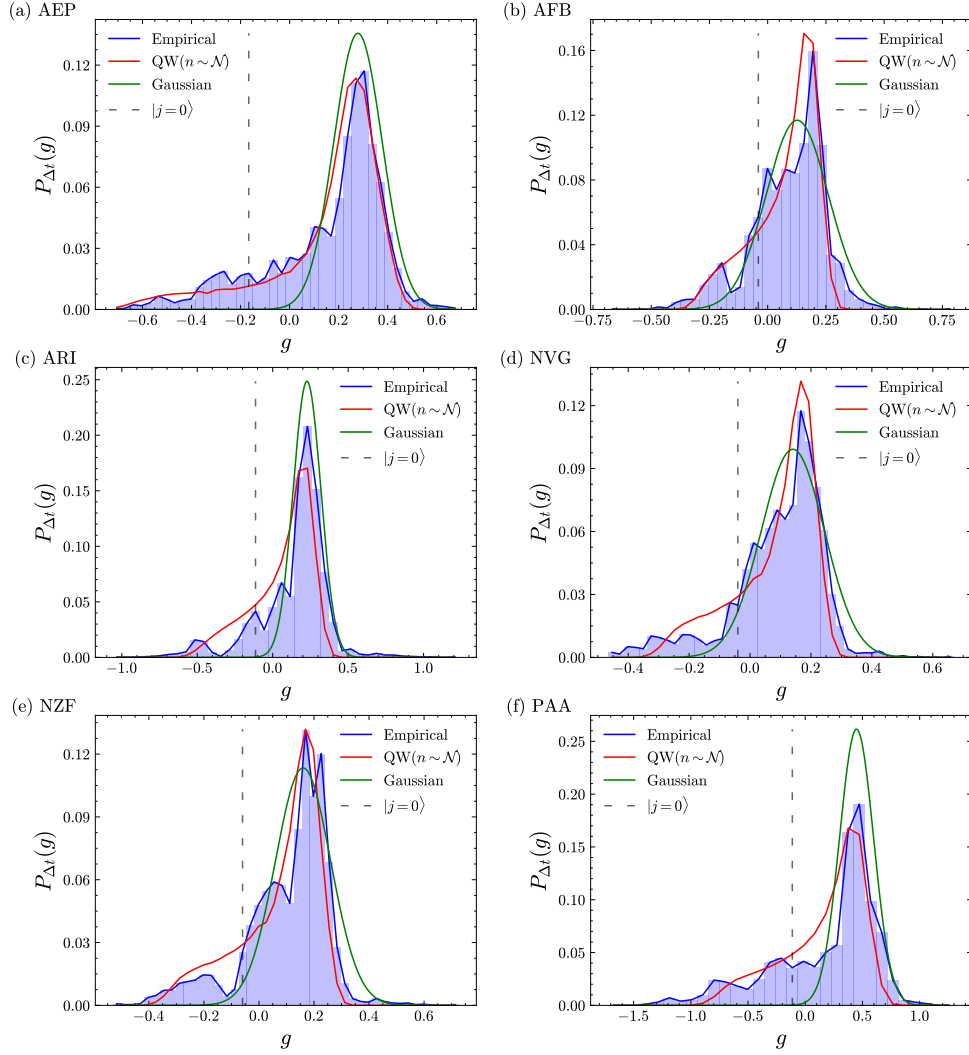


Figure 10: Quantum walk and Gaussian fits of the logarithmic return distribution $P_{\Delta t}(g)$ exhibiting considerable asymmetry (with $\Delta t = 2$ trading years) for the six selected assets of Fig. 4. The number of time steps n in the quantum walk is distributed according to a normal distribution $\mathcal{N}(\mu = 100, \sigma^2 = 15^2)$. The vertical dashed line corresponds to the initial position $|j = 0\rangle$ of the quantum walk.

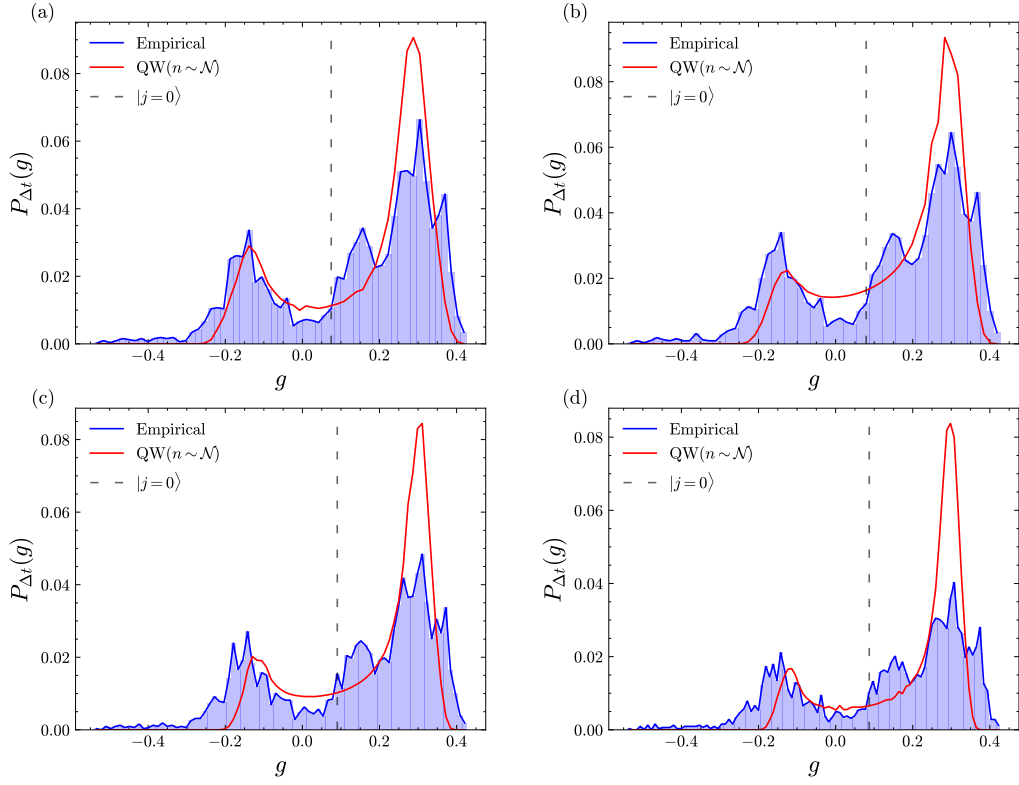


Figure 11: Quantum walk fit of the logarithmic return distribution $P_{\Delta t}(g)$ (with $\Delta t = 2$ trading years) for the asset DMO. The number of time steps n is distributed according to a normal distribution (a) $\mathcal{N}(\mu = 100, \sigma^2 = 15^2)$, (b) $\mathcal{N}(\mu = 120, \sigma^2 = 18^2)$, (c) $\mathcal{N}(\mu = 140, \sigma^2 = 21^2)$, and (d) $\mathcal{N}(\mu = 160, \sigma^2 = 24^2)$. The vertical dashed line corresponds to the initial position $|j = 0\rangle$ of the quantum walk.

Capturing their characteristics is particularly relevant for option pricing models, where accurate representations of return distributions over long time horizons are key to assessing derivative values and associated risks. In particular, a bimodal distribution can be associated with a combination of substantial losses and gains, having significant implications for long-term risk management. We used a quantum walk model to characterize the bimodality and asymmetry in these long-term return distributions, leveraging the quantum interference effects intrinsic to its dynamics to capture these empirical features. Although there is still room to improve the quality of the quantum walk fits, they reflect the observed behavior substantially better than a Gaussian distribution, and can provide insights into the underlying dynamics of asset price evolution. By identifying regions within the coin parameter space that can be associated with bimodal and asymmetric return distributions, we can relate the quantum walk parameters to different classes of long-term asset price dynamics.

In future work, the analysis can be extended to larger data sets, and more refined fitting strategies can be explored to further improve the quality of the quantum walk fits. Nevertheless, at large time scales, such as those of two trading years, achieving a perfect characterization of the return distributions is inherently challenging. A larger data set would also enable a more detailed analysis of the distribution and clustering of the fitted quantum walk parameters, for example by examining whether assets from different economic sectors occupy distinct regions of parameter space. Another interesting research question is whether there is a discernible difference in the quantum walk parameters for the return distributions of composite assets and of single assets. The analysis presented in this work contains both classes, but the sample sizes are too small for a detailed comparative analysis. A further line for future research lies in the inclusion of decoherence effects into the quantum walk algorithm to investigate how return distributions evolve from smaller to larger time scales. Indeed, by including decoherence effects, one can generate asymmetric probability distributions with heavier tails than a Gaussian distribution, which offers applications for modeling short-term return distributions.

Appendix A. Data

Table A.2 provides an overview of the analyzed assets, presenting their ticker, full name, sector, industry, and the end and start date of the analyzed time series. The data set was obtained from <https://finance.yahoo.com/> on October 14, 2024.

Ticker	Full name	Sector	Industry	Start date	End date
6599.KL	Aeon Co. (M) Bhd.	Consumer Cyclical	Department Stores	2000-01-03	2024-10-14
AALI.JK	PT Astra Agro Lestari Tbk	Consumer Defensive	Farm Products	2001-04-05	2024-10-14
AAOI	Applied Optoelectronics, Inc.	Technology	Communication Equipment	2013-09-26	2024-10-11
AB	AllianceBernstein Holding L.P.	Financial Services	Asset Management	1994-10-19	2024-10-11
ACV	Virtus Diversified Income & Convertible Fund	Financial Services	Asset Management	2015-05-21	2024-10-11
ADDYY	adidas AG	Consumer Cyclical	Footwear & Accessories	2006-05-31	2024-10-11

Ticker	Full name	Sector	Industry	Start date	End date
ADX	Adams Diversified Equity Fund, Inc.	Financial Services	Asset Management	1994-10-19	2024-10-11
AEP	American Electric Power Company, Inc.	Utilities	Utilities - Regulated Electric	1994-10-19	2024-10-11
AFB	AllianceBernstein National Municipal Income Fund, Inc.	Financial Services	Asset Management	2002-01-29	2024-10-11
AFSI	AmTrust Financial Services, Inc.	Financial Services	Insurance - Property & Casualty	2006-11-13	2018-12-10
AJX	Great Ajax Corp.	Real Estate	REIT - Mortgage	2015-02-13	2024-10-11
AM	Antero Midstream Corporation	Energy	Oil & Gas Midstream	2017-05-04	2024-10-11
AMCX	AMC Networks Inc.	Communication Services	Entertainment	2011-06-16	2024-10-11
AMG	Affiliated Managers Group, Inc.	Financial Services	Asset Management	1997-11-21	2024-10-11
AMX	América Móvil, S.A.B. de C.V.	Communication Services	Telecom Services	2001-02-12	2024-10-11
ANY	Sphere 3D Corp.	Financial Services	Capital Markets	2013-08-12	2024-10-11
ARI	Apollo Commercial Real Estate Finance, Inc.	Real Estate	REIT - Mortgage	2009-09-24	2024-10-11
AWK	American Water Works Company, Inc.	Utilities	Utilities - Regulated Water	2008-04-23	2024-10-11
BABA	Alibaba Group Holding Limited	Consumer Cyclical	Internet Retail	2014-09-19	2024-10-11
DMO	Western Asset Mortgage Opportunity Fund Inc.	Financial Services	Asset Management	2010-02-24	2024-10-11
EVTC	EVERTEC, Inc.	Technology	Software - Infrastructure	2013-04-12	2024-10-11
GBAB	Guggenheim Taxable Municipal Bond & Investment Grade Debt Trust	Financial Services	Asset Management	2010-10-28	2024-10-11
IGI	Western Asset Investment Grade Opportunity Trust Inc.	Financial Services	Asset Management	2009-07-01	2024-10-11
ISL	Aberdeen Israel Fund, Inc.	Financial Services	Asset management	2009-09-08	2018-04-30
MTGE	MTGE Investment Corp.	Real Estate	REIT - Mortgage	2011-08-04	2018-09-17
NSA	National Storage Affiliates Trust	Real Estate	REIT - Industrial	2015-04-22	2024-10-11

Ticker	Full name	Sector	Industry	Start date	End date
NVG	Nuveen AMT-Free Municipal Credit Income Fund	Financial Services	Asset Management	2002-09-12	2024-10-11
NZF	Nuveen Municipal Credit Income Fund	Financial Services	Asset Management	2001-10-03	2024-10-11
PAA	Plains All American Pipeline, L.P.	Energy	Oil & Gas Midstream	1998-11-18	2024-10-11
SAVE	Spirit Airlines, Inc.	Industrials	Airlines	2011-05-26	2024-10-11
TEAM	Atlassian Corporation	Technology	Software - Application	2015-12-09	2024-10-11

Table A.2: Overview of the analyzed assets, including their ticker, full name, sector, industry, and the start and end date of the analyzed time series.

Declaration of Generative AI and AI-assisted technologies in the writing process

During the preparation of this work, the authors used ChatGPT in order to enhance the readability of this work. After using this tool, the authors reviewed and edited the content as needed and take full responsibility for the content of the publication.

Declaration of competing interest

The authors declare that they have no known competing financial interests or personal relationships that could have appeared to influence the work reported in this paper.

Acknowledgment

This project was conducted with the support of the Special Research Fund of Ghent University (projects BOF/DOC/2023/103 and BOF/BAF/4y/24/1/018).

References

- [1] L. Bachelier, Theorie de la spéculation, Annales Scientifiques de l'École Normale Supérieure 3 (17) (1900) 21–86.
- [2] B. Mandelbrot, The variation of the prices of cotton, wheat, and railroad stocks, and of some financial rates, Fractals and Scaling in Finance: Discontinuity, Concentration, Risk. Selecta Volume E (1997) 419–443.
- [3] B. Mandelbrot, The Variation of Certain Speculative Prices, The Journal of Physics 36 (4) (1963) 394–419.
- [4] V. Ziemann, Physics and Finance, Undergraduate Lecture Notes in Physics, Springer International Publishing, 2021.
- [5] F. Black, M. Scholes, The Pricing of Options and Corporate Liabilities, Journal of Political Economy 81 (3) (1973) 637–654.
- [6] X. Gabaix, Power Laws in Economics and Finance, Annual Review of Economics 1 (1) (2009) 255–294.
- [7] P. Gopikrishnan, M. Meyer, L. N. Amaral, H. E. Stanley, Inverse cubic law for the distribution of stock price variations, The European Physical Journal B-Condensed Matter and Complex Systems 3 (2) (1998) 139–140.
- [8] P. Gopikrishnan, V. Plerou, L. A. N. Amaral, M. Meyer, H. E. Stanley, Scaling of the distribution of fluctuations of financial market indices, Physical Review E 60 (5) (1999) 5305.
- [9] W. Yuan, S. Lai, The CEV model and its application to financial markets with volatility uncertainty, Journal of Computational and Applied Mathematics 344 (2018) 25–36.
- [10] L. C. G. Rogers, Arbitrage with fractional Brownian motion, Mathematical finance 7 (1) (1997) 95–105.
- [11] S. Rostek, R. Schöbel, A note on the use of fractional Brownian motion for financial modeling, Economic Modelling 30 (2013) 30–35.

- [12] S. G. Kou, A jump-diffusion model for option pricing, *Management science* 48 (8) (2002) 1086–1101.
- [13] R. C. Merton, Option pricing when underlying stock returns are discontinuous, *Journal of financial economics* 3 (1-2) (1976) 125–144.
- [14] F. Hanson, J. Westman, Jump-Diffusion Stock Return Models in Finance: Stochastic Process Density with Uniform-Jump Amplitude, *Proceedings of the 15th International Symposium on Mathematical Theory of Networks and Systems* (01 2002).
- [15] R. Cont, M. Potters, J.-P. Bouchaud, Scaling in stock market data: stable laws and beyond, in: *Scale Invariance and Beyond: Les Houches Workshop, March 10–14, 1997*, Springer, 1997, pp. 75–85.
- [16] E. Eberlein, U. Keller, Hyperbolic distributions in finance, *Bernoulli* (1995) 281–299.
- [17] O. E. Barndorff-Nielsen, Normal inverse Gaussian distributions and stochastic volatility modelling, *Scandinavian Journal of statistics* 24 (1) (1997) 1–13.
- [18] R. C. Blattberg, N. J. Gonedes, A comparison of the stable and student distributions as statistical models for stock prices, in: *Perspectives on promotion and database marketing: The collected works of Robert C Blattberg*, World Scientific, 2010, pp. 25–61.
- [19] J. Laherrere, D. Sornette, Stretched exponential distributions in nature and economy: “fat tails” with characteristic scales, *The European Physical Journal B-Condensed Matter and Complex Systems* 2 (1998) 525–539.
- [20] Y. Malevergne, V. Pisarenko, D. Sornette, Empirical distributions of stock returns: between the stretched exponential and the power law?, *Quantitative Finance* 5 (4) (2005) 379–401.
- [21] S. Dutta, T. K. Powdel, Modeling long term return distribution and nonparametric market risk estimation, *Sankhya B* 85 (Suppl 1) (2023) 257–289.
- [22] X. Meng, J.-W. Zhang, H. Guo, Quantum Brownian motion model for the stock market, *Physica A: Statistical Mechanics and its Applications* 452 (2016) 281–288.
- [23] D. B. Madan, E. Seneta, The variance gamma (VG) model for share market returns, *Journal of business* (1990) 511–524.
- [24] K. Kiyono, Z. R. Struzik, Y. Yamamoto, Criticality and phase transition in stock-price fluctuations, *Physical review letters* 96 (6) (2006) 068701.
- [25] K. Kiyono, Z. R. Struzik, Y. Yamamoto, Power law and its transition in the slow convergence to a Gaussian in the S&P500 index, in: *Practical Fruits of Econophysics: Proceedings of the Third Nikkei Econophysics Symposium*, Springer, 2006, pp. 67–71.
- [26] Ç. Tuncay, D. Stauffer, Power laws and Gaussians for stock market fluctuations, *Physica A: Statistical Mechanics and its Applications* 374 (1) (2007) 325–330.
- [27] S. De Backer, L. E. C. Rocha, J. Ryckebusch, K. Schoors, On the potential of quantum walks for modeling financial return distributions, *Physica A: Statistical Mechanics and its Applications* 657 (2025) 130215.
- [28] T. D. Mackay, S. D. Bartlett, L. T. Stephenson, B. C. Sanders, Quantum walks in higher dimensions, *Journal of Physics A: Mathematical and General* 35 (12) (2002) 2745.
- [29] T. A. Brun, H. A. Carteret, A. Ambainis, Quantum random walks with decoherent coins, *Physical Review A* 67 (3) (2003) 032304.
- [30] T. A. Brun, H. A. Carteret, A. Ambainis, Quantum walks driven by many coins, *Physical Review A* 67 (5) (2003) 052317.
- [31] A. Romanelli, R. Siri, G. Abal, A. Auyuanet, R. Donangelo, Decoherence in the quantum walk on the line, *Physica A: Statistical Mechanics and its Applications* 347 (2005) 137–152.
- [32] A. Romanelli, G. Hernández, Quantum walks: Decoherence and coin-flipping games, *Physica A: Statistical Mechanics and its Applications* 390 (6) (2011) 1209–1220.
- [33] M. N. Jayakody, A. Nanayakkara, Transfiguration of Quantum Walks on a line, *arXiv preprint arXiv:1809.00505* (2018).
- [34] N. I. Ishak, S. V. Muniandy, W. Y. Chong, Entropy analysis of the discrete-time quantum walk under bit-flip noise channel, *Physica A: Statistical Mechanics and its Applications* 584 (2021) 126371.
- [35] Y. Aharonov, L. Davidovich, N. Zagury, Quantum random walks, *Physical Review A* 48 (2) (1993) 1687.
- [36] J. Kempe, Quantum random walks: an introductory overview, *Contemporary Physics* 44 (4) (2003) 307–327.
- [37] S. E. Venegas-Andraca, Quantum walks: a comprehensive review, *Quantum Information Processing* 11 (5) (2012) 1015–1106.
- [38] C. M. Chandrashekar, R. Srikanth, R. Laflamme, Optimizing the discrete time quantum walk using a SU (2) coin, *Physical Review A* 77 (3) (2008) 032326.
- [39] R. Cont, Empirical properties of asset returns: stylized facts and statistical issues, *Quantitative finance* 1 (2) (2001) 223.
- [40] P. Liu, Y. Zheng, Precision Measurement of the Return Distribution Property of the Chinese Stock Market Index, *Entropy* 25 (1) (2022) 36.
- [41] J. Y. Campbell, A. W. Lo, A. C. MacKinlay, R. F. Whitelaw, The econometrics of financial markets, *Macroeconomic Dynamics* 2 (4) (1998) 559–562.

- [42] R. Mantegna, H. Stanley, *An Introduction to Econophysics: Correlations and Complexity in Finance*, Vol. 53, Cambridge University Press, 2000.
- [43] B. Sharma, S. Agrawal, M. Sharma, D. Bisen, R. Sharma, *Econophysics: A brief review of historical development, present status and future trends*, arXiv preprint arXiv:1108.0977 (2011).
- [44] B. W. Silverman, *Using kernel density estimates to investigate multimodality*, *Journal of the Royal Statistical Society: Series B (Methodological)* 43 (1) (1981) 97–99.
- [45] J. A. Hartigan, P. M. Hartigan, *The dip test of unimodality*, *The annals of Statistics* (1985) 70–84.
- [46] D. W. Müller, G. Sawitzki, *Excess mass estimates and tests for multimodality*, *Journal of the American Statistical Association* 86 (415) (1991) 738–746.
- [47] A. Siffer, P.-A. Fouque, A. Termier, C. Largouët, *Are your data gathered?*, in: *Proceedings of the 24th ACM SIGKDD International Conference on Knowledge Discovery & Data Mining*, 2018, pp. 2210–2218.
- [48] A. Gupta, A. J. Onumanyi, S. Ahlawat, Y. Prasad, V. Singh, A. M. Abu-Mahfouz, *Dat: A robust discriminant analysis-based test of unimodality for unknown input distributions*, *Pattern Recognition Letters* 182 (2024) 125–132.
- [49] S. J. Russell, P. Norvig, *Artificial Intelligence: A Modern Approach*, 3rd Edition, Pearson Education, Inc., Upper Saddle River, New Jersey, 2010.
- [50] D. Orrell, *Quantum Economics and Finance: An Applied Mathematics Introduction*, Panda Ohana Publishing, 2020.
- [51] D. Orrell, *A quantum walk model of financial options*, *Wilmott* 2021 (112) (2021) 62–69.
- [52] D. Orrell, *Money, Magic, and How to Dismantle a Financial Bomb: Quantum Economics for the Real World*, Icon Books Ltd, 39–41 North Road, London N7 9DP, 2022.